

Consistent quantum treatments of non-convex kinetic energies

C. Koliofoti, M. A. Javed and R.-P. Riwar¹

¹*Peter Grünberg Institute, Theoretical Nanoelectronics,
Forschungszentrum Jülich, D-52425 Jülich, Germany*

The task of finding a consistent relationship between a quantum Hamiltonian and a classical Lagrangian is of utmost importance for basic, but ubiquitous techniques like canonical quantization and path integrals. Nonconvex kinetic energies (which appear, e.g., in Wilczek and Shapere's classical time crystal, or nonlinear capacitors) pose a fundamental problem: the Legendre transformation is ill-defined, and the more general Legendre-Fenchel transformation removes nonconvexity essentially by definition. Arguing that such anomalous theories follow from suitable low-energy approximations of well-defined, harmonic theories, we show that seemingly inconsistent Hamiltonian and Lagrangian descriptions can both be valid, depending on the coupling strength to a dissipative environment. Essentially there occurs a dissipative phase transition from a non-convex Hamiltonian to a convex Lagrangian regime, involving exceptional points in imaginary time. This resolves apparent inconsistencies and provide computationally efficient methods to treat anomalous, nonconvex kinetic energies.

Introduction. – Canonical quantization (CQ) [1] and the path integral (PI) formalism [2], are indispensable tools for modern quantum theory. Both methods rely on a well-defined correspondence between a classical Lagrangian L and a quantum Hamiltonian H , which is usually obtained from the Legendre transformation [3]. But there are various important cases where the Legendre transformation is ill-defined [4] [5]. The velocity-momentum relationship is non-invertible if the mass tensor has zero eigenvalues, requiring alternative quantization procedures [6–9] which have recently been subject to controversy [10–12]. Shapere and Wilczek's classical time crystal is based on the notion of nonconvex kinetic energies in L [13], whose consistent quantization presents an unresolved challenge to this day [14, 15], where in particular "branched quantization" methods [16–18] have been criticized [19].

This work focuses on non-convex kinetic energies in the *Hamiltonian*. Such Hamiltonians appear in the quantum circuit context as nonlinear, anomalous capacitors, either in the form of electrostatically coupled polarizer objects [20, 21], polarizing materials (ferroelectrics) [22–27], quantum phase slip junctions [28–36], or auxiliary charge qubits [37, 38]. While the Hamiltonian is here known, the path to a corresponding Lagrangian is nonetheless of fundamental importance, in order to model quantum circuit hardware of ever increasing complexity [39, 40] with the circuit quantization approach [41–43], and in order to efficiently describe dissipation via PI [44]. Reconstructing a valid Lagrangian from a non-convex Hamiltonian is problematic for the same reason as for classical time crystals [19]: while the Legendre-Fenchel transformation formally applies to non-convex functions, it replaces them with their convex hull [45]. While for quantum phase slip junctions, methods have been proposed to circumvent nonconvexity [36, 46], a general, proper understanding of non-convex kinetic energies, and their efficient PI treatment, remain an unresolved fundamental problem.

We study models where anomalous kinetic energies arise from suitable low-energy approximations of regular, harmonic theories. This allows us to derive seemingly inconsistent H and L , where (in qualitative, but not quantitative, agreement with Ref. [19]) the Lagrangian completely misses the phase transition from convex to non-convex. Notably, we find that both results can be correct – in complementary regimes. We show that nonconvexity in H coincides with *exceptional points* in imaginary time PI. Including a dissipative environment, we identify two regimes. At low dissipation, imaginary time paths reach the exceptional points, such that the non-convex H is correct, whereas the low-energy approximation of L fails due to adiabaticity breaking. Conversely, sufficiently strong dissipation smoothen out the imaginary time paths, restoring adiabaticity, validating the convex solution due to L . Overall, we find that inconsistent Hamiltonian and Lagrangian treatments both have their validity depending on dissipation strength, and in doing so, we find a computationally efficient PI treatment of anomalous kinetic energies in the presence of dissipation.

Our work connects in unexpected ways to other ongoing research thrusts. Exceptional points are currently being explored as a means to describe topological phase transitions in open, driven quantum systems [47–63]. While the transition from convex to non-convex energies occurs without gap closing in the real-time energy spectrum, it can be related to a deeply topological feature when mapping to imaginary times. The prediction of dissipative phase transitions dates back to over four decades [64, 65]. But its experimental verification [66–71] and some theoretical aspects [72–76] remain controversial to this day. The dissipative phase transition we report on here (effectively destroying non-convexity) is similar to the localization phase transition known from the spin-boson model [77] and the Schmid-Bulgadaev phase transition [64, 65] in the Caldeira-Leggett model, but, crucially, relies on a conceptually different mecha-

nism, in that the energy barrier between two minimas is not renormalized by high frequency paths, but effectively disappears due to the environment-induced path adiabaticity. Finally, our approach allows for a well-defined conceptional access to consistent quantum treatments of classical time crystals, to be studied in the future.

Minimal toy model. – Before presenting our arguments in their most general form, we begin for simplicity with a concrete minimal toy model. While the here developed concepts hold independent of the specific physical platform, we stick throughout this work to the language of quantum circuits, where the pair of canonically conjugate operators are the Cooper pair charge N and superconducting phase ϕ . The velocity $\dot{\phi}$ corresponds to the voltage across the capacitor, as per second Josephson relation.

Consider a circuit comprised of a parallel shunt of capacitor with an inductor. In order to render the capacitor effectively nonlinear, we include an intrinsic pseudo-spin degree of freedom (similar to Ref. [78]). The Hamiltonian and corresponding Lagrangian of the full system are

$$H = \hat{T}(N) + V(\phi) \quad L = \hat{T}^*(\dot{\phi}) - V(\phi) \quad (1)$$

with the kinetic energies $\hat{T}(N) = (N + \lambda\sigma_z)^2 / (2c) + \gamma\sigma_x$ and $\hat{T}^*(\dot{\phi}) = c\dot{\phi}^2/2 - \lambda\dot{\phi}\sigma_z - \gamma\sigma_x$. The two are related via standard Legendre transformation in $\dot{\phi}$, since the kinetic energies are quadratic. The pseudo-spin is represented by ordinary Pauli matrices $\sigma_{x,z}$. The shunt inductor is expressed with the potential energy term $V(\phi)$ (which is, e.g., $\sim \phi^2$ for a linear inductor, or $\sim \cos(\phi)$ for a Josephson junction [79]). The bare capacitor has a capacitance c (in units of inverse energy). Physically, the pseudo-spin can be regarded as a quantum dipole moment (e.g., a single electron trapped in a double quantum dot), where the voltage across the capacitor $\sim \dot{\phi}$ leads to a detuning $\sim \lambda\dot{\phi}$ and γ expresses a tunneling process between the two dipole configurations, see Fig. 1(b).

Since the pseudo-spin is not Legendre transformed, L is strictly speaking only ‘half-classical’ [80]. Leaving the pseudo-spin quantum provides an energy gap $\sim \gamma$ in both representations, which allows us to perform a low-energy approximation in Born-Oppenheimer style, eliminating the fast pseudo-spin. This yields a scalar low-energy theory (where for scalar kinetic energies, we drop the hat notation, $\hat{T} \rightarrow T$). For H , we choose the energetically lowest eigenvalues with respect to spin [black line in Fig. 1(c)],

$$\hat{T}(N) \approx T(N) = \frac{1}{2c}N^2 - \sqrt{\lambda^2 N^2/c^2 + \gamma^2}. \quad (2)$$

For the Lagrangian on the other hand, we have to select the highest eigenvalue [81] [black line in Fig. 1(d)],

$$\hat{T}^*(\dot{\phi}) \approx T^*(\dot{\phi}) = \frac{c}{2}\dot{\phi}^2 + \sqrt{\lambda^2 \dot{\phi}^2 + \gamma^2}. \quad (3)$$

The scalar kinetic energy T in Eq. (2) undergoes a phase transition at the critical point $\gamma_0 = \lambda^2/c$. For $\gamma < \gamma_0$

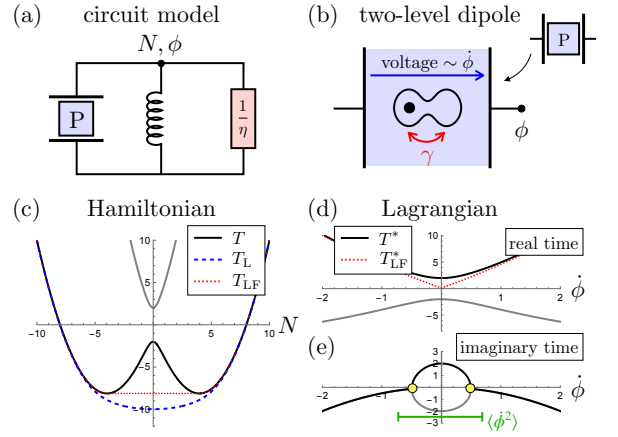


FIG. 1. Main findings of this work, illustrated by simple toy model. (a) Nonlinear capacitor (with polarizing element/material P) is shunted with an inductor and resistor. (b) Quantum dipole with two charge states (coupled with rate γ) interacting with the voltage across the capacitor. The Hamiltonian and Lagrangian descriptions of the device in (b) can be understood in terms of eigenvalues (black and grey lines) of $\hat{T}(N)$ (c) and $\hat{T}^*(\dot{\phi})$ (d), respectively, $\hat{T}^*(i\dot{\phi})$ for imaginary time (e). The black lines mark the low-energy approximation. Blue dashed and red dotted lines correspond to Legendre-, respectively Legendre-Fenchel-transformed kinetic energies (see main text). (e) Exceptional points (marked with yellow dots) are relevant if PI voltage noise (green bar) is sufficiently large. In (e) only real part of the spectrum is plotted. In (c,d,e), the y-axis is energy in units of $1/c$, and $\lambda = 4$, $c\gamma = 2$.

($\gamma > \gamma_0$), the kinetic energy is *non-convex* (convex), qualitatively resembling the known behaviour of ferroelectric materials [22–27]. This transition can be probed, e.g., by the heat capacity, $C_v = \beta^2 \partial_\beta^2 \ln(Z)$ with β the inverse temperature ($k_B = 1$), and the partition function $Z = \text{tr}[e^{-\beta H}]$. For a linear inductive shunt, $V(\phi) = \phi^2/(2l)$, the heat capacity can be computed analytically in the limit $\gamma \gg 1/\beta \gg 1/l$ [82]. Before and after the transition, we find $C_v = 1$, whereas at the critical point ($\gamma = \gamma_0$) we have $C_v = 3/4$ (due to $T \sim N^4$).

In contrast to T , the low-energy Lagrangian kinetic energy T^* , Eq. (3), always remains convex. In fact, for low voltages $\dot{\phi} \approx 0$, we can always approximate it as harmonic, $T^* \approx c_{\text{eff}}\dot{\phi}^2$. A trace of the phase transition remains in the form of a renormalization of the effective capacitance $c_{\text{eff}} = c + \lambda^2/\gamma$. This renormalization crosses over from weak before the transition ($\gamma \gg \gamma_0$), $c_{\text{eff}} \approx c$, and strong after the transition ($\gamma \ll \gamma_0$), $c_{\text{eff}} \approx \lambda^2/\gamma \gg c$.

Because T^* is always convex, we can in principle apply a standard Legendre transformation directly for the Lagrangian low-energy theory. The kinetic energy from that transformation, denoted as $T_L(N)$, *cannot* possibly be consistent with the direct low-energy $T(N)$ in Eq. (2), as it is convex by definition. We can even get a third (yet again inconsistent) version of the low-energy kinetic

energy in H , by applying the Legendre-Fenchel transformation to the original, nonconvex $T(N)$, arriving at an intermediary Lagrangian with $T_{\text{LF}}^*(\dot{\phi})$, and applying it a second time to get back to the Hamiltonian, now with kinetic energy $T_{\text{LF}}(n)$. T_{L} and T_{LF} are qualitatively similar (both removing the nonconvexity), but only the former remains smooth, see Fig. 1(c) and (d) (in alignment with Ref. [19]).

With a full model at our disposal, we could simply argue that only T is correct (at least under the assumptions so far stated), while T_{L} and T_{LF} must be rejected. While T_{LF} can (at least in the present context) be discarded as a mere mathematical exercise, the inconsistency between T and T_{L} is nonetheless surprising as both follow from a low-energy approximation due to an energy gap. In particular, had we given the convex low-energy L in Eq. (3) as starting point, we would not have found the correct, non-convex low-energy H . To our knowledge, no work in the existing literature warns about the possibility that CQ for an anharmonic, but strictly convex T^* in L could provide a wrong Hamiltonian.

Imaginary time path integrals. – Therefore, it is crucial to understand what exactly went wrong for T_{L} . To address this, we turn to the PI approach. Since we consider finite temperatures, we turn to imaginary times [83], expressing the partition function for the full system as

$$Z = \oint \mathcal{D}\phi \text{tr}_\sigma \left[\mathcal{T} e^{\int_0^\beta d\tau [\hat{T}^*(i\dot{\phi}_\tau) - V(\phi_\tau)]} \right], \quad (4)$$

where the notation $\oint \mathcal{D}\phi$ represents the ordinary functional integral over all possible paths ϕ_τ with periodic boundary conditions $\phi_\beta = \phi_0$ [44]. Note that we only transformed the pair of N, ϕ into classical variables $\dot{\phi}, \phi$, while leaving the pseudo-spin quantum [82], which is why there is a separate trace over the pseudo-spin degrees of freedom ($\text{tr}_\sigma[\dots]$), and the Lagrangian 'time evolution' requires imaginary time ordering (\mathcal{T}).

For imaginary times ($t \rightarrow -i\tau$), the voltage gets an additional prefactor i , such that the eigenvalues of \hat{T}^* are $-c\dot{\phi}_\tau^2/c \pm \sqrt{\gamma^2 - \lambda^2\dot{\phi}_\tau^2}$. Consequently, when $\dot{\phi}_\tau$ passes the threshold value γ/λ , the system exhibits *exceptional points* as a function of $\dot{\phi}$. In contrast, both the Hamiltonian and *real-time* Lagrangian always have a well-defined direct energy gap with respect to the pseudo-spin, independent of $\dot{\phi}$. This explains the failure of T_{L} : we cannot in general perform a low-energy approximation on L , because the energy gap does not persist for imaginary times. We can find precise conditions for when exactly the exceptional points become important, by comparing their onset with the magnitude of PI fluctuations of $\dot{\phi}$, see Fig. 1(e). The noise power spectrum of $\dot{\phi}_\tau$ evaluated for paths generated by the bare system [82],

$$S_{\dot{\phi}}(\omega_k) = \int_0^\beta d\tau e^{i\omega_k(\tau-\tau')} \left\langle \dot{\phi}_\tau \dot{\phi}_{\tau'} \right\rangle_{\text{paths}} = \frac{\omega_k^2}{c\omega_k^2 + 1/l}, \quad (5)$$

where $\omega_k = 2\pi k/\beta$ are the ordinary Matsubara frequencies. The high frequency tail is constant white noise, and as such, the voltage variance diverges, $\langle \phi_\tau^2 \rangle \rightarrow \infty$. However, the system contains a natural UV cutoff due to the energy gap γ , a fact that can be shown via a time-dependent basis transformation [82]. This cutoff regularizes voltage fluctuations felt by the pseudo-spin to the finite value $\langle \dot{\phi}_\tau^2 \rangle \sim \gamma/c$. Inserting this expectation value into the condition for the appearance of exceptional points, $\gamma^2 = \lambda^2 \langle \dot{\phi}_\tau^2 \rangle$, we get a critical value of $\gamma \sim \lambda^2/c$. Crucially, this coincides with the critical value for γ , at which the system transitions from convex to non-convex, allowing us to connect this phase transition with the onset of exceptional points in imaginary time PI.

The issue is thus a question of adiabaticity: below the phase transition, voltage fluctuations are sufficiently weak for exceptional point to be irrelevant, justifying an adiabatic approximation in Eq. (4), replacing the operator L by the eigenvalue with real part closest zero, $-c\dot{\phi}_\tau^2/2 + \sqrt{\gamma^2 - \lambda^2\dot{\phi}_\tau^2} \approx -c_{\text{eff}}\dot{\phi}_\tau^2/2$ [84]. At and above the phase transition, however, PI voltage fluctuations increase to the extent that the exceptional points are reached, and adiabaticity of the paths ϕ_τ is broken.

Including dissipation. – Surprisingly, the low-energy Lagrangian in Eq. (3) can nonetheless be valid above the transition in a different regime. Shunting the circuit with an Ohmic resistance R , see Fig. 1(a), the noise power spectrum changes to [44]

$$S_{\dot{\phi}}(\omega_k) = \frac{\omega_k^2}{c\omega_k^2 + |\omega_k|/(2\pi\eta) + 1/l}, \quad (6)$$

with the damping coefficient $1/\eta = R_Q/R$ (R_Q being the resistance quantum). Remaining in the regime $1/\beta \gg 1/l$, we get a transition from weak to strong dissipation when the damping surpasses the critical value $1/\eta \gtrsim c\gamma$. Above this point, the voltage noise goes from $\langle \dot{\phi}_\tau^2 \rangle \sim \gamma/c$ to the much smaller value $\langle \dot{\phi}_\tau^2 \rangle \sim \eta\gamma^2$. Here, adiabaticity with respect to exceptional points is guaranteed as long as $1/\eta \gtrsim \lambda^2$. Combining the non-convexity condition $c\gamma \sim \lambda^2$, with the above strong dissipation and adiabaticity conditions, we get $1/\eta \gtrsim \lambda^2, c\gamma$. In this regime, there is therefore no restriction on the relative magnitude of the quantities λ^2 and $c\gamma$, meaning that we can cross the point $\lambda^2 \sim c\gamma$ without infringing the exceptional points. The adiabatic, low-energy $L \approx c_{\text{eff}}\dot{\phi}^2/2 - V(\phi)$ in Eq. (3) thus retains its validity. However, this also means that the point $\lambda^2 \sim c\gamma$ no longer marks a phase transition. For nonzero $1/\eta$, the heat capacity is sensitive to the capacitance. We find for $\beta/(\eta c_{\text{eff}}) > 1$ [82]

$$C_v \approx 1 + \frac{2\pi^2\eta c_{\text{eff}}}{\beta}. \quad (7)$$

Consequently, what used to be measurable as a second order phase transition in the absence of dissipation (where

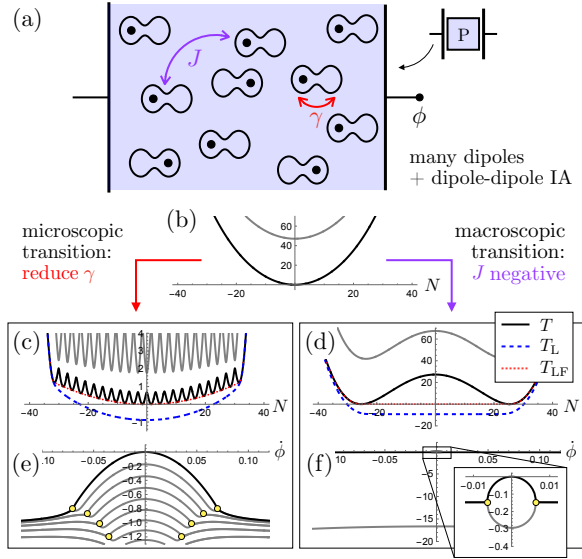


FIG. 2. Generalization to a model with many dipoles (a). For sufficiently large γ and $J > 0$, the low-energy spectrum of $\hat{T}(N)$ is convex (b). By either reducing γ , or rendering $J < 0$, the model undergoes a microscopic (c), respectively macroscopic (d) phase transition, with a nonconvex ground state (black lines). Legendre- and Legendre-Fenchel-transformed kinetic energies are again drawn in blue dashed and red dotted lines in (c,d). The imaginary time eigenspectrum of $\hat{T}^*(i\phi)$ is shown in (e,f), exhibiting exceptional points (yellow dots) correlating with the number of minima of the nonconvex T from the corresponding Hamiltonian (c,d). In (b-f), the y-axis is energy, again in units of $1/c$, and $\lambda = 3$, $S = 21/2$. The other parameters are $c\gamma = 20$ (b,d,f), $c\gamma = 0.1$ (c,e), and $cJ = 0.01$ (b,c,e), $cJ = -1.5$ (d,f).

C_v dips from 1 to $3/4$ at the critical point), now turns into a smooth crossover from weakly to strongly renormalized capacitance, visible in C_v .

Generalization. – The above concepts and findings can be generalized. Consider a coupling to a many-body system (referred to as ‘polarizer’ from here on),

$$\hat{T}(N) = \frac{1}{2c} (N + \Lambda)^2 + \Gamma, \quad \hat{T}^*(\phi) = \frac{c}{2} \phi^2 - \phi \Lambda - \Gamma, \quad (8)$$

where operator Λ is proportional to the total polarizer dipole moment, and operator Γ describes its intrinsic dynamics [85]. The linear coupling in ϕ is generic, since for first principle modelling of electronic degrees of freedom, any externally applied voltage enters the Hamiltonian linearly. Thus, for imaginary times, $\phi \rightarrow i\dot{\phi}$, the emergence of exceptional points is inescapable as ϕ increases.

Regarding non-convexity, this general model can provide two types of transitions. To see this, notice that the first part ($\sim 1/c$) provides as the eigenspectrum a set of parabolas as a function of N , shifted by the eigenvalues of Λ . A finite Γ leads to a hybridization, and thus an avoided crossing of the parabolas. For sufficiently large coupling, the spectrum gets smoothened out in N -space,

leaving in general a convex function behind. This is the same type of phase transition as in the toy model presented above, now generalized for a large, macroscopic polarizer. We call it the ‘microscopic’ transition, as the nonconvex features here resolve the individual, quantized dipole moments. The second type can be thought of as a ‘macroscopic’ phase transition, where the intrinsic dynamics within Γ do not only lead to hybridization, but also include a mechanism that energetically favors strongly separated, macroscopic states.

These two transition types can be illustrated by an explicit polarizer model, larger than above toy model, but still simple enough to make quantitative predictions. We take $\Lambda = \lambda S_z$ and $\Gamma = \gamma S_x + JS_z^2$, where $S_{x,z}$ are the components of a large pseudo-spin of size $S \gg 1$. Such models have been extensively studied in the past in the context of spin-squeezed states [86] [87]. This model can be derived from an ensemble of K two-level dipole moments, $\sigma_{x,z} \rightarrow \sigma_{x,y}^{(k)}$ ($k = 1, \dots, K$), and is exactly diagonalizable for fairly large spins [82]. The model and the two transition types are illustrated in Fig. 2.

We again compare the T that results from the lowest eigenvalue of H_{full} , with T_L (the indirect calculation via Legendre transforming T^* , the highest eigenvalue of L_{full}), and with T_{LF} (again, a double Legendre-Fenchel-transformed T), see Fig. 2(b,c,d). Above the transition (γ largest energy scale, J small but positive), we can describe the low-energy physics again with a well-defined effective capacitance $c_{\text{eff}} \approx c + S\lambda^2/\gamma$. The microscopic transition (lowering γ below the critical value) qualitatively resembles the two-level toy model. In particular, the low-energy T_L again features a smooth crossover from weakly to strongly renormalized effective capacitance, relevant again for the strongly dissipative regime, where the formula in Eq. (7) still holds.

In contrast, the macroscopic phase transition occurs as soon as we cross over to small but negative J , where the system quickly reaches a tipping point, due to the competition between the γS_x and JS_z^2 terms. With their respective scaling $\sim S\gamma$ and $\sim S^2J$, we see that when $|J| > \gamma/S$, the system topples towards a state maximizing (instead of minimizing) S_z^2 . In the thermodynamic limit $S \rightarrow \infty$ this happens for arbitrarily small, negative J . The Legendre-transformed T_L then features an almost flat energy with respect to N , see Fig. 2(d), representing a nearly diverging effective capacitance. This feature follows from a residual avoided crossing between the $S_z = -S$ and $S_z = +S$ states in the eigenspectrum of \hat{T}^* , which for $|J| > \gamma/S$ is exponentially suppressed. If β and $1/\eta$ are sufficiently large, we can still perform the adiabatic approximation (avoiding exceptional points) even in this extreme regime. We thus witness a first order phase transition (instead of a cross over) due to the sudden increase of the effective capacitance. For moderate dissipation however, the exceptional point cannot be avoided any more. Contrary to all other cases dis-

cussed above, which allow for the various analytic results presented throughout this work, this last case requires a numerical evaluation of the path integral. Importantly though, such a calculation is still tractable: while the gap between the two states involved in the exceptional point formation is (exponentially) small, there still exists a finite gap to the higher states, see Fig. 2(f). This requires the evaluation of Eq. (4) truncated to a two-by-two model – ultimately mapping back to the toy model discussed above. Regarding truncation, we generally remark that the number of minima in the Hamiltonian, Fig. 2(c,d), directly correlates with the number of relevant low-energy exceptional points the imaginary time Lagrangian, Fig. 2(e,f). This means that PI calculations with many minimas for weak to moderate $1/\eta$ are numerically more challenging to handle than few minima.

Finally, we comment on the usefulness of T_{LF} for the macroscopic model. Here, it actually agrees with T_L to a much higher degree (compare blue dashed and red dotted lines in Fig. 2). In particular, both kinetic energy version are useful to capture phase transitions (or the lack thereof) in c_{eff} in the strongly dissipative regime.

Conclusions and outlook. – With explicit models realizing nonconvex kinetic energies in H , we have clarified the usefulness of various low-energy approximations on the Hamiltonian and Lagrangian level, as well as their correspondence (or lack thereof) via the Legendre and Legendre-Fenchel transformations. We conclude that it is perfectly acceptable to have inconsistent low-energy L and H , as they are applicable in complementary regimes of strong and weak dissipation, respectively, marking a dissipative phase transition. Our framework allows for efficient computation of observables (often even analytically) with PI methods, where the presence of exceptional points in imaginary time can be linked to nonconvexity in real time.

As a future research direction, we note that while the here considered models always yielded convex Lagrangian kinetic energies, there is no fundamental principle forbidding non-convexity, thus realizing classical time crystals [13]. In the light of incompatibility issues between L and H that are currently being debated in this field [14–19], we expect that our microscopic approach could resolve those issues, and naturally provide access to the quantum treatment of classical time crystals, without the need to develop new quantization methods.

We warmly thank David P. DiVincenzo for fruitful discussions. This work has been funded by the German Federal Ministry of Education and Research within the funding program Photonic Research Germany under the contract number 13N14891.

-
- [1] F. Schwabl, *Quantum Mechanics*, 4th ed. (Springer, Berlin, Germany, 2007).
 - [2] A. Zee, *Quantum field theory in a nutshell*, second edition ed. (Princeton University Press, 2010).
 - [3] Strictly speaking, the connection between H and L for PI is the Fourier transformation, and not the Legendre transformation. The two are only equivalent for *harmonic* kinetic energies.
 - [4] In line with the previous footnote, the conventional PI approach loses validity for *any* anharmonic kinetic energy, an issue that is well-known in the relativistic community, see, e.g., Ref. [5] and references therein.
 - [5] T. Padmanabhan, *The European Physical Journal C* **78**, 563 (2018).
 - [6] P. G. Bergmann and J. H. M. Brunings, *Rev. Mod. Phys.* **21**, 480 (1949).
 - [7] L. Faddeev and R. Jackiw, *Phys. Rev. Lett.* **60**, 1692 (1988).
 - [8] J. D. Brown, *Universe* **8**, 10.3390/universe8030171 (2022).
 - [9] A. Parra-Rodriguez and I. L. Egusquiza, *Quantum* **8**, 1466 (2024).
 - [10] M. Rymarz and D. P. DiVincenzo, *Phys. Rev. X* **13**, 021017 (2023).
 - [11] I. L. Egusquiza and A. Parra-Rodriguez, *Phys. Rev. X* **15**, 028001 (2025).
 - [12] D. P. DiVincenzo and M. Rymarz, *Phys. Rev. X* **15**, 028002 (2025).
 - [13] A. Shapere and F. Wilczek, *Phys. Rev. Lett.* **109**, 160402 (2012).
 - [14] L. Zhao, P. Yu, and W. Xu, *Modern Physics Letters A* **28**, 1350002 (2013), <https://doi.org/10.1142/S0217732313500028>.
 - [15] J. Dai, A. J. Niemi, and X. Peng, *New Journal of Physics* **22**, 085006 (2020).
 - [16] M. Henneaux, C. Teitelboim, and J. Zanelli, *Phys. Rev. A* **36**, 4417 (1987).
 - [17] A. Shapere and F. Wilczek, *Phys. Rev. Lett.* **109**, 200402 (2012).
 - [18] A. G. Choudhury and P. Guha, *Modern Physics Letters A* **34**, 1950263 (2019), <https://doi.org/10.1142/S0217732319502638>.
 - [19] H.-H. Chi and H.-J. He, *Nuclear Physics B* **885**, 448 (2014).
 - [20] W. A. Little, *Phys. Rev.* **134**, A1416 (1964).
 - [21] A. Hamo, A. Benyamini, I. Shapir, I. Khivrich, J. Waissman, K. Kaasbjerg, Y. Oreg, F. von Oppen, and S. Ilani, *Nature* **535**, 395 (2016).
 - [22] R. Landauer, *Collect. Phenom.* **2**, 167 (1976).
 - [23] G. Catalan, D. Jiménez, and A. Gruverman, *Nature Materials* **14**, 137 (2015).
 - [24] K. Ng, S. J. Hillenius, and A. Gruverman, *Solid State Communications* **265**, 12 (2017).
 - [25] M. Hoffmann, A. I. Khan, C. Serrao, Z. Lu, S. Salahuddin, M. Pešić, S. Slesazek, U. Schroeder, and T. Mikołajick, *J. Appl. Phys.* **123**, 184101 (2018).
 - [26] I. Luk'yanchuk, Y. Tikhonov, A. Sené, A. Razumnaya, and V. M. Vinokur, *Commun. Phys.* **2**, 22 (2019).
 - [27] M. Hoffmann, S. Slesazek, U. Schroeder, and T. Mikołajick, *Nature Electronics* **3**, 504 (2020).
 - [28] N. Giordano, *Phys. Rev. Lett.* **61**, 2137 (1988).

- [29] A. Bezryadin, C. Lau, and M. Tinkham, *Nature* **404**, 971 (2000).
- [30] C. N. Lau, N. Markovic, M. Bockrath, A. Bezryadin, and M. Tinkham, *Phys. Rev. Lett.* **87**, 217003 (2001).
- [31] H. P. Büchler, V. B. Geshkenbein, and G. Blatter, *Phys. Rev. Lett.* **92**, 067007 (2004).
- [32] J. E. Mooij and Y. V. Nazarov, *Nature Physics* **2**, 169 (2006).
- [33] O. V. Astafiev, L. B. Ioffe, S. Kafanov, Y. A. Pashkin, K. Y. Arutyunov, D. Shahar, O. Cohen, and J. S. Tsai, *Nature* **484**, 355 (2012).
- [34] S. E. de Graaf, S. T. Skacel, T. Hönl-Deccrinis, R. Shaikhaidarov, H. Rotzinger, S. Linzen, M. Ziegler, U. Hübner, H. G. Meyer, V. Antonov, E. Il'ichev, A. V. Ustinov, A. Y. Tzalenchuk, and O. V. Astafiev, *Nature Physics* **14**, 590 (2018).
- [35] R. S. Shaikhaidarov, K. H. Kim, J. W. Dunstan, I. V. Antonov, S. Linzen, M. Ziegler, D. S. Golubev, V. N. Antonov, E. V. Il'ichev, and O. V. Astafiev, *Nature* **608**, 45 (2022).
- [36] C. Koliofoti and R.-P. Riwar, *npj Quantum Information* **9**, 125 (2023).
- [37] T. Herrig, J. H. Pixley, E. J. König, and R. P. Riwar, *npj Quantum Information* **9**, 116 (2023).
- [38] T. Herrig, C. Koliofoti, J. H. Pixley, E. J. König, and R.-P. Riwar, *Phys. Rev. B* **111**, L201104 (2025).
- [39] F. Arute, K. Arya, R. Babbush, D. Bacon, J. C. Bardin, R. Barends, R. Biswas, S. Boixo, F. G. S. L. Brandao, D. A. Buell, B. Burkett, Y. Chen, Z. Chen, B. Chiaro, R. Collins, W. Courtney, A. Dunsworth, E. Farhi, B. Foxen, A. Fowler, C. Gidney, M. Giustina, R. Graff, K. Guerin, S. Habegger, M. P. Harrigan, M. J. Hartmann, A. Ho, M. Hoffmann, T. Huang, T. S. Humble, S. V. Isakov, E. Jeffrey, Z. Jiang, D. Kafri, K. Kechedzhi, J. Kelly, P. V. Klimov, S. Knysh, A. Korotkov, F. Kostritsa, D. Landhuis, M. Lindmark, E. Lucero, D. Lyakh, S. Mandrà, J. R. McClean, M. McEwen, A. Megrant, X. Mi, K. Michielsen, M. Mohseni, J. Mutus, O. Naaman, M. Neeley, C. Neill, M. Y. Niu, E. Ostby, A. Petukhov, J. C. Platt, C. Quintana, E. G. Rieffel, P. Roushan, N. C. Rubin, D. Sank, K. J. Satzinger, V. Smelyanskiy, K. J. Sung, M. D. Trevithick, A. Vainsencher, B. Villalonga, T. White, Z. J. Yao, P. Yeh, A. Zalcman, H. Neven, and J. M. Martinis, *Nature* **574**, 505 (2019).
- [40] See <https://www.ibm.com/blogs/research/2020/09/ibm-quantum-roadmap/> (2020).
- [41] G. Burkard, R. H. Koch, and D. P. DiVincenzo, *Phys. Rev. B* **69**, 064503 (2004).
- [42] U. Vool and M. Devoret, *International Journal of Circuit Theory and Applications* **45**, 897 (2017).
- [43] R. P. Riwar and D. P. DiVincenzo, *npj Quantum Information* **8**, 36 (2022).
- [44] A. Altland and B. D. Simons, *Condensed Matter Field Theory* (Cambridge University Press, Cambridge, UK, 2010).
- [45] Specifically, the Lagrangian obtained from the Legendre-Fenchel-transformed Hamiltonian becomes in general non-smooth, and a second application does not recover the original non-convex Hamiltonian, but a deformed, convexified variant.
- [46] J. Ulrich and F. Hassler, *Phys. Rev. B* **94**, 094505 (2016).
- [47] K. Ding, G. Ma, Z. Q. Zhang, and C. T. Chan, *Phys. Rev. Lett.* **121**, 085702 (2018).
- [48] R.-P. Riwar, *Phys. Rev. B* **100**, 245416 (2019).
- [49] F. E. Öztürk, T. Lappe, G. Hellmann, J. Schmitt, J. Klaers, F. Vewinger, J. Kroha, and M. Weitz, *Science* **372**, 88 (2021), <https://www.science.org/doi/pdf/10.1126/science.abe9869>.
- [50] Q. Liao, C. Leblanc, J. Ren, F. Li, Y. Li, D. Solnyshkov, G. Malpuech, J. Yao, and H. Fu, *Phys. Rev. Lett.* **127**, 107402 (2021).
- [51] A. V. Hlushchenko, D. V. Novitsky, V. I. Shcherbinin, and V. R. Tuz, *Journal of Optics* **23**, 125002 (2021).
- [52] S. Xia, C. Danieli, Y. Zhang, X. Zhao, H. Lu, L. Tang, D. Li, D. Song, and Z. Chen, *APL Photonics* **6**, 126106 (2021), <https://pubs.aip.org/aip/app/article-pdf/doi/10.1063/5.0069633/14055975/126106.1.online.pdf>.
- [53] K. Ding, C. Fang, and G. Ma, *Nature Reviews Physics* **4**, 745 (2022).
- [54] M. A. Javed, J. Schwibbert, and R.-P. Riwar, *Phys. Rev. B* **107**, 035408 (2023).
- [55] F. K. Kunst, E. Edvardsson, J. C. Budich, and E. J. Bergholtz, *Physical Review Letters* **121**, 026808 (2018).
- [56] K. Kawabata, K. Shiozaki, M. Ueda, and M. Sato, *Physical Review X* **9**, 041015 (2019).
- [57] W. D. Heiss, *Journal of Physics A: Mathematical and General* **37**, 2455 (2004).
- [58] W. D. Heiss, *Journal of Physics A: Mathematical and Theoretical* **45**, 444016 (2012).
- [59] H. C. Wu, L. Jin, and Z. Song, *Phys. Rev. B* **100**, 155117 (2019).
- [60] I. Mandal and E. J. Bergholtz, *Phys. Rev. Lett.* **127**, 186601 (2021).
- [61] E. J. Bergholtz, J. C. Budich, and F. K. Kunst, *Rev. Mod. Phys.* **93**, 015005 (2021).
- [62] J. Avila, F. Peñaranda, E. Prada, P. San-Jose, and R. Aguado, *Communications Physics* **2**, 10.1038/s42005-019-0231-8 (2019).
- [63] P. San-Jose, J. Cayao, E. Prada, and R. Aguado, *Scientific Reports* **6**, 10.1038/srep21427 (2016).
- [64] A. Schmid, *Phys. Rev. Lett.* **51**, 1506 (1983).
- [65] S. A. Bulgadaev, *JETP Letters* **39**, 315 (1984).
- [66] A. Murani, N. Bourlet, H. le Sueur, F. Portier, C. Altimiras, D. Esteve, H. Grabert, J. Stockburger, J. Ankerhold, and P. Joyez, *Phys. Rev. X* **10**, 021003 (2020).
- [67] P. J. Hakonen and E. B. Sonin, *Phys. Rev. X* **11**, 018001 (2021).
- [68] A. Murani, N. Bourlet, H. le Sueur, F. Portier, C. Altimiras, D. Esteve, H. Grabert, J. Stockburger, J. Ankerhold, and P. Joyez, *Phys. Rev. X* **11**, 018002 (2021).
- [69] R. Kuzmin, N. Mehta, N. Grabon, R. A. Mencia, A. Burshtein, M. Goldstein, and V. E. Manucharyan, *arXiv:2304.05806*.
- [70] M. Houzet, T. Yamamoto, and L. I. Glazman, *Phys. Rev. B* **109**, 155431 (2024).
- [71] A. Burshtein and M. Goldstein, *PRX Quantum* **5**, 020323 (2024).
- [72] K. Masuki, H. Sudo, M. Oshikawa, and Y. Ashida, *Phys. Rev. Lett.* **129**, 087001 (2022).
- [73] T. Sépulcre, S. Florens, and I. Snyman, *Phys. Rev. Lett.* **131**, 199701 (2023).
- [74] K. Masuki, H. Sudo, M. Oshikawa, and Y. Ashida, *Phys. Rev. Lett.* **131**, 199702 (2023).
- [75] L. Giacomelli and C. Ciuti, *Nature Communications* **15**, 5455 (2024).
- [76] O. Kashuba and R.-P. Riwar, *Phys. Rev. B* **110**, 184505 (2024).

- (2024).
- [77] A. J. Leggett, S. Chakravarty, A. T. Dorsey, M. P. A. Fisher, A. Garg, and W. Zwerger, *Rev. Mod. Phys.* **59**, 1 (1987).
 - [78] B. A. Placke, T. Pluecker, J. Splettstoesser, and M. R. Wegewijs, *Phys. Rev. B* **98**, 085307 (2018).
 - [79] For simplicity, this work will mostly focus on linear inductors, where the problem of non-convex $T(N)$ could in principle be avoided by performing a Legendre transformation on $V(\phi)$ instead of $T(N)$, similar in spirit to Ref. [46]. But our goal is to provide a theory that works independent of whether the inductive shunt is linear or nonlinear.
 - [80] For readers who are uneasy with the notion of a Legendre transformation where some degrees of freedom remain quantum (here the pseudo-spin), we refer to the PI treatment further below in the main text for clarification.
 - [81] The reason for selecting the highest, and not the lowest eigenvalue becomes clear when considering the system in a thermal Gibbs state (for which we will use imaginary times), see further below.
 - [82] See Supplemental Material for more details.
 - [83] Many of our conclusions also apply to real-time PI methods, but we leave a detailed discussion of this topic for follow-up research.
 - [84] Via analytic continuation from imaginary times back to real times, we now understand why in Eq. (3) we had to choose the higher, and not the lower eigenenergy.
 - [85] Both Λ and Γ are Hermitean operators.
 - [86] A. G. Rojo, *Phys. Rev. A* **68**, 013807 (2003).
 - [87] As an aside: for $J > 0$, if S_z remains sufficiently small compared to S , we can approximate the dynamics as an effective Josephson effect, $S_z \sim n$, $S_x \sim \cos(\varphi)$ with $[n, \varphi] = i$. Incidentally, this results in a model that has been recently proposed to exist when coupling charge islands to charge qubits, resulting in a quasiperiodic nonlinear capacitor [37, 38].

Supplemental Material: Consistent quantum treatments of anharmonic kinetic energies

C. Koliofoti, M. A. Javed and R.-P. Riwar¹

¹*Peter Grünberg Institute, Theoretical Nanoelectronics,
Forschungszentrum Jülich, D-52425 Jülich, Germany*

This supplemental material provides additional information on the following subjects. In Sec. [SI](#) we detail the calculation of the heat capacitance reported on in the main text, both without and with a resistive shunt. Section [SII](#) presents the 'partial' path integral approach, wherein the charge and phase operators are turned into classical coordinates, whereas the intrinsic capacitor degrees of freedom remain quantum. In Sec. [SIII](#) we define and compute the path integral noise power spectra for the voltage ϕ in imaginary time, which is used in the main text to estimate adiabaticity with respect to exceptional points. Section [SIV](#) details the imaginary time basis transformation which allows us to deduce a high frequency cutoff in the noise power spectrum. In Sec. [SV](#) we show how the large pseudo-spin model in the second part of the main text follows from a microscopic model with an ensemble of two-level quantum dipole moments.

SI. CALCULATION OF HEAT CAPACITY

A. Zero dissipation

The partition function can be directly related to the density of states, which we assume to satisfy a low-energy power law (we rescaled the energy spectrum such that the ground state is at zero energy)

$$Z = \text{tr} [e^{-\beta H}] = \int_0^\infty dE \rho(E) e^{-\beta E} \sim \int_0^\infty dE E^\kappa e^{-\beta E} = \beta^{-\kappa-1} \Gamma(\kappa + 1) \quad (\text{S.1})$$

where Γ is the Gamma function. The heat capacity, defined as $C_v = \beta^2 \partial_\beta^2 \ln(Z)$, then straightforwardly yields

$$C_v = 1 + \kappa. \quad (\text{S.2})$$

We thus need to find the power law of the density of states.

Take a low energy Hamiltonian with kinetic and potential energies

$$H = T(N) + V(\varphi). \quad (\text{S.3})$$

We assume (as in the main text) a harmonic potential energy $V(\varphi) = \phi^2/2l$. As for the kinetic energy, we assume that at low energies, it satisfies a power law behaviour $T(N) \sim |N|^\alpha$. Then, the low-energy density of states in the limit $l \rightarrow \infty$ can be computed by the convolution formula [\[38\]](#)

$$\rho(E) \sim \int_0^E dE' \frac{1}{\sqrt{E-E'}} \rho_0(E') \quad (\text{S.4})$$

where ρ_0 is the density of states for the kinetic term only, assuming equidistant distribution of the eigenvalues N ,

$$\rho_0 \sim E^{1-\frac{1}{\alpha}}. \quad (\text{S.5})$$

With the above convolution formula, we get

$$\rho \sim E^{\frac{1}{\alpha}-\frac{1}{2}}, \quad (\text{S.6})$$

and, consequently, arrive at

$$C_v = \frac{1}{2} + \frac{1}{\alpha}. \quad (\text{S.7})$$

For the kinetic energy of the two-level model in the main text,

$$T(N) = \frac{N^2}{2c} - \sqrt{\frac{\lambda^2 N^2}{c^2} + \gamma^2}$$

the system undergoes a phase transition at $\gamma_0 = \lambda^2/c$. Before and after the transition, the power law is $\alpha = 2$, yielding

$$C_v = 1. \quad (\text{S.8})$$

At the transition, the quadratic term vanishes, and we are left with a low-energy kinetic term that scales with $\alpha = 4$, such that

$$C_v = \frac{3}{4}, \quad (\text{S.9})$$

as stated in the main text.

B. Finite dissipation

We here compute the expression for the heat capacity in the presence of an Ohmic resistor. This problem can be expressed in terms of standard path integral methods, where the partition function in Fourier space is given as [44]

$$Z \sim \lim_{k_{\text{co}} \rightarrow \infty} \int d\phi_0 e^{-\beta \frac{\phi_0^2}{2l}} \prod_{k=1}^{k_{\text{co}}} \int d\phi_{kr} \int d\phi_{ki} e^{-\beta \sum_{k=1}^{k_{\text{co}}} \left(\frac{c \left(\frac{2\pi k}{\beta} \right)^2}{2} + \frac{1}{4\pi\eta} \frac{2\pi k}{\beta} + \frac{1}{2l} \right) (\phi_{kr}^2 + \phi_{ki}^2)} \quad (\text{S.10})$$

with the Matsubara frequencies $\omega_k = 2\pi k/\beta$, where for $k > 0$, we take into account the fact that the Fourier components are complex, $\phi_k = \phi_{kr} + i\phi_{ki}$, i.e., the transformation from imaginary time to frequency space is

$$\phi_\tau = \phi_0 + \frac{1}{\sqrt{2}} \sum_{k=1}^{k_{\text{co}}} \left[(\phi_{kr} + i\phi_{ki}) e^{i \frac{2\pi}{\beta} k\tau} + (\phi_{kr} - i\phi_{ki}) e^{-i \frac{2\pi}{\beta} k\tau} \right]. \quad (\text{S.11})$$

Note that this partition function is strictly speaking not convergent in the limit $k_{\text{co}} \rightarrow \infty$, due to the divergent UV tail (which is why we explicitly keep the cutoff k_{co} here). But the resulting heat capacity is well-defined for $k_{\text{co}} \rightarrow \infty$, yielding

$$C_v = \frac{1}{2} \sum_{k=-\infty}^{\infty} \left[\left(\frac{\frac{\beta}{c\eta} |k| + 2\beta^2 \frac{1}{lc}}{4\pi^2 k^2 + \frac{\beta}{c\eta} |k| + \frac{\beta^2}{lc}} \right)^2 - \frac{2\frac{\beta^2}{lc}}{4\pi^2 k^2 + \frac{\beta}{c\eta} |k| + \frac{\beta^2}{lc}} \right].$$

In the limit $1/l \rightarrow 0$, this sum yields

$$C_v = \left(\frac{\beta}{4\pi^2 c\eta} \right)^2 \psi^{(1)} \left(\frac{\beta}{4\pi^2 c\eta} \right), \quad (\text{S.12})$$

where $\psi^{(1)}$ is the first derivative of the Digamma function. Assuming asymptotically large arguments, this function is approximated as $\psi^{(1)}(z) \approx 1/z + 1/(2z^2)$, yielding Eq. (7) in the main text.

SII. PARTIAL PATH INTEGRAL METHOD

Here we derive the form of the partition function as shown in Eq. (4) in the main text. We begin with the definition of a partition function

$$Z = \text{tr} [e^{-\beta H}], \quad (\text{S.13})$$

where H is the Hamiltonian of the full system (Eq. (1) in the main text). Since the full system is comprised of two subsystems: one with charge/phase degree of freedom and the other with the pseudo-spin degree of freedom, the total trace over the system can be written as the combination of traces over the two subsystems. Hence, we can write

$$Z = \text{tr}_\sigma [\text{tr}_\phi [e^{-\beta H}]], \quad (\text{S.14})$$

where tr_σ is the trace over the pseudo-spin degree of freedom and tr_ϕ is the trace over the charge/phase degree of freedom.

Our goal will be to write the trace tr_ϕ as a path integral, therefore we first replace this trace with the eigenstates $(|\phi\rangle)$ of the phase operator, to get

$$Z = \int d\phi \text{tr}_\sigma [\langle \phi | e^{-\beta H} | \phi \rangle]. \quad (\text{S.15})$$

Once we have the expression $\langle \phi | e^{-\beta H} | \phi \rangle$, we can use the procedure similar to the one used to derive the path integral formulation of quantum mechanics [44]. We begin by breaking the exponential of the Hamiltonian into M components

$$\langle \phi | \left(e^{-\frac{\beta}{M} H} \right)^M | \phi \rangle = \langle \phi | \underbrace{e^{-\Delta\tau H} \dots e^{-\Delta\tau H}}_{M \text{ times}} | \phi \rangle, \quad (\text{S.16})$$

where we have defined $\Delta\tau = \beta/M$. Eventually we will take the limit $M \rightarrow \infty$, but for now we take it to be large enough so that we can use the following approximation

$$e^{-\Delta\tau H} = e^{-\Delta\tau \hat{T}(N)} e^{-\Delta\tau V(\phi)} + \mathcal{O}(\Delta\tau^2). \quad (\text{S.17})$$

Writing the exponential in the above factorized form allows us to diagonalize the kinetic energy term and the potential energy term independently. To use this independence we insert the resolution of identity (\mathcal{I}) in the expression $\langle \phi | e^{-\beta H} | \phi \rangle$

$$\langle \phi | \left(e^{-\frac{\beta}{M} H} \right)^M | \phi \rangle = \langle \phi | \mathcal{I}_M e^{-\Delta\tau \hat{T}(N)} e^{-\Delta\tau V(\phi)} \mathcal{I}_{M-1} \dots \mathcal{I}_1 e^{-\Delta\tau \hat{T}(N)} e^{-\Delta\tau V(\phi)} | \phi \rangle, \quad (\text{S.18})$$

where

$$\mathcal{I}_j = \int d\phi_j \int dN_j |\phi_j\rangle \langle \phi_j| N_j\rangle \langle N_j| \otimes \mathcal{I}_\sigma,$$

the subscript j helps to differentiate the different phase and charge variables originating from different resolutions of identity, and \mathcal{I}_σ is the identity in the pseudo-spin space.

Using the expression $\langle \phi | N \rangle = \langle N | \phi \rangle^* = e^{iN\phi}/\sqrt{2\pi}$, we can write

$$Z = \text{tr}_\sigma \left[\int \prod_{j=1}^M d\phi_j \int \prod_{j=1}^M \frac{dN_j}{2\pi} \mathcal{T} \exp \left(-\Delta\tau \sum_{j=1}^M \left[\hat{T}(N_j) + V(\phi_{j-1}) - iN_j \frac{\phi_j - \phi_{j-1}}{\delta\tau} \right] \right) \right], \quad (\text{S.19})$$

with the constraint that $\phi_0 = \phi_M = \phi$. Here, we have also used the time ordering operator \mathcal{T} because even if the charge and phase operators have now been replaced with their eigenvalues, the pseudo-spin degree of freedom is still quantum, and one has to arrange the quantum operators in the correct order of increasing imaginary time. We now use the specific form of $\hat{T}(N) = (N + \lambda\sigma_z)^2/2c + \gamma\sigma_x$, and perform the Gaussian integrals over the variables N_j to get

$$Z = \text{tr}_\sigma \left[\int \prod_{j=1}^M \frac{cd\phi_j}{\delta\tau} \mathcal{T} \exp \left(-\Delta\tau \sum_{j=1}^M \left[\frac{c}{2} \left(\frac{\phi_j - \phi_{j-1}}{\delta\tau} \right)^2 + i\lambda \frac{\phi_j - \phi_{j-1}}{\delta\tau} \sigma_z + \gamma\sigma_x + V(\phi_{j-1}) \right] \right) \right]. \quad (\text{S.20})$$

Finally we take the limit $M \rightarrow \infty$, while keeping $M\Delta\tau = \beta$ constant. This allows us to replace the sum $\sum_{j=1}^M \Delta\tau$ with the integral $\int_0^\beta d\tau$, and to also make the following replacements

$$\begin{aligned} \frac{\phi_j - \phi_{j-1}}{\Delta\tau} &\rightarrow \partial_\tau \phi \equiv \dot{\phi}_\tau \\ V(\phi_{j-1}) &\rightarrow V(\phi(\tau)). \end{aligned}$$

Hence the partition function becomes

$$Z = \text{tr}_\sigma \left[\oint D\phi \mathcal{T} \exp \left(- \int_0^\beta d\tau \left[\frac{c}{2} \dot{\phi}_\tau^2 + i\lambda \dot{\phi}_\tau \phi \sigma_z + \gamma\sigma_x + V(\phi) \right] \right) \right], \quad (\text{S.21})$$

where

$$\oint D\phi = \lim_{M \rightarrow \infty} \prod_{j=1}^M \int \frac{cd\phi_j}{\Delta\tau}, \quad (\text{S.22})$$

is the integral measure and the closed integral sign \oint represents the fact that the integration is being performed over all the paths (in imaginary time) for which $\phi(\tau=0) = \phi(\tau=\beta)$. To bring this in the form of Eq. (4), we interchange the order of the path integral and the trace over the pseudo-spin degree of freedom. We also note that if we replace t in the expression of $\hat{T}^*(\dot{\phi})$ (Eq. (1) in the main text) by $-i\tau$, we get

$$T^*(i\partial_\tau \phi) = -\frac{c}{2} \dot{\phi}_\tau^2 - i\lambda \dot{\phi}_\tau \sigma_z - \gamma\sigma_x. \quad (\text{S.23})$$

Therefore, the final form of the partition function is

$$Z = \oint \mathcal{D}\phi \text{tr}_\sigma \left[\mathcal{T} e^{\int_0^\beta d\tau [\hat{T}^*(i\dot{\phi}_\tau) - V(\phi_\tau)]} \right]. \quad (\text{S.24})$$

SIII. NOISE POWER SPECTRUM OF BARE LC RESONATOR

In the main text, we provide the imaginary-time voltage noise power spectrum for the bare LC resonator system either with [Eq. (6)] or without [Eq. (5)] an Ohmic resistor. We here derive these expressions. We introduce the notation for averaging over paths of said LC resonator as follows [in analogy to the ordinary path integral treatment, see Eq. (S.10) above]

$$\langle \bullet \rangle_{\text{path}} \equiv \lim_{k_{\text{co}} \rightarrow \infty} \frac{\prod_{k=0}^{k_{\text{co}}} \int d\phi_k e^{-\beta \left(\frac{c\omega_k^2}{2} + \frac{\omega_k}{4\pi\eta} + \frac{1}{2l} \right) |\phi_k|^2} \langle \bullet \rangle}{\prod_{k=0}^{k_{\text{co}}} \int d\phi_k e^{-\beta \left(\frac{c\omega_k^2}{2} + \frac{\omega_k}{4\pi\eta} + \frac{1}{2l} \right) |\phi_k|^2}}. \quad (\text{S.25})$$

The above is a shorthand notation of the path integral introduced in Eq. (S.10), where for $k > 0$, the integral $\int d\phi_k$ goes over the 2D complex plane, $\int d\phi_{k\tau} \int d\phi_{ki}$. Plugging in Eq. (S.11) for ϕ_τ , we can now calculate with ease the expectation value for

$$\left\langle \dot{\phi}_\tau \dot{\phi}_{\tau'} \right\rangle_{\text{path}} = \frac{1}{2} \sum_{k=1}^{\infty} S_k \left[e^{i\omega_k(\tau-\tau')} + e^{-i\omega_k(\tau-\tau')} \right] \quad (\text{S.26})$$

with S_k as given in Eq. (6) of the main text. Equation (5) follows of course from (6) by setting $1/\eta = 0$.

SIV. TIME DEPENDENT BASIS TRANSFORMATION AND INTRINSIC UV CUTOFF

In the main text, we argue that the energy gap γ provides an intrinsic UV cutoff. We here explain and demonstrate this statement. The object we will be looking at is the partition function Z , defined in Eq. (4) of the main text. In fact, we consider it explicitly for the two-level toy model presented in the first part of the main text, and take the ratio with respect to the bare LC resonator partition function Z_0 (i.e., removing the additional quantum dipole). This quantity can be expressed as

$$\frac{Z}{Z_0} = \text{tr}_\sigma \left[\left\langle \mathcal{T} e^{-\int_0^\beta d\tau (i\lambda \dot{\phi}_\tau \sigma_z + \gamma \sigma_x)} \right\rangle_{\text{path}} \right] \quad (\text{S.27})$$

where we use the notation for the average taken over the bare paths as given above, in Eq. (S.25). Now, there are two steps involved.

The first step consists of applying a time-dependent basis transformation to the above path integral expression. We start from the time-ordered propagator in Eq. (S27), and rewrite it explicitly in K discrete time slices of length $\Delta\tau = \beta/K$,

$$\mathcal{T} e^{-\int_0^\beta d\tau (i\lambda \dot{\phi}_\tau \sigma_z + \gamma \sigma_x)} = \lim_{K \rightarrow \infty} \prod_{j=1}^K e^{-\Delta\tau (i\lambda \dot{\phi}_{\tau_j} \sigma_z + \gamma \sigma_x)} = \prod_{j=1}^K e^{-\Delta\tau i\lambda \dot{\phi}_{\tau_j} \sigma_z} e^{-\Delta\tau \gamma \sigma_x}, \quad (\text{S.28})$$

where it is important to keep the product \prod ordered with ascending k index. The terms $e^{-\Delta\tau \gamma \sigma_x}$ can be recast into the form of a time-dependent basis transformation

$$U_j = e^{-j\Delta\tau \gamma \sigma_x} \quad (\text{S.29})$$

such that

$$\prod_{j=1}^K e^{-\Delta\tau i\lambda \dot{\phi}_{\tau_j} \sigma_z} e^{-\Delta\tau \gamma \sigma_x} = U_K \prod_{j=1}^K e^{-\Delta\tau i\lambda \dot{\phi}_{\tau_j} U_j^{-1} \sigma_z U_j}. \quad (\text{S.30})$$

U_j is not unitary, due to imaginary times. Going back to continuous time, we get

$$\mathcal{T} e^{-\int_0^\beta d\tau (i\lambda \dot{\phi}_\tau \sigma_z + \gamma \sigma_x)} = e^{-\beta \gamma \sigma_x} \mathcal{T} e^{-i\lambda \int_0^\beta d\tau \dot{\phi}_\tau e^{\tau \gamma \sigma_x} \sigma_z e^{-\tau \gamma \sigma_x}}. \quad (\text{S.31})$$

At this stage, we already see that $\dot{\phi}_\tau$ is convoluted with $e^{\pm\gamma\tau}$ terms, indicating already on a qualitative level, that γ likely acts as a cutoff energy scale for fluctuations in $\dot{\phi}_\tau$.

In a second step, we make this intuitive insight quantitative, by expanding in λ , and evaluating the correlators. For illustrative purposes, we here focus on leading order (second order in λ), where we get

$$\left\langle \text{tr}_\sigma \left[\mathcal{T} e^{-\int_0^\beta d\tau (i\lambda \dot{\phi}_\tau \sigma_z + \gamma \sigma_x)} \right] \right\rangle_{\text{path}}^{(2)} = -\lambda^2 e^{\beta \gamma} \int_0^\beta d\tau \int_0^\tau d\tau' \left\langle \dot{\phi}_\tau \dot{\phi}_{\tau'} \right\rangle_{\text{path}} \left[e^{2(\tau-\tau'-\beta)\gamma} + e^{-2(\tau-\tau')\gamma} \right]. \quad (\text{S.32})$$

Out of those two terms, the second one is the leading one, such that we arrive at

$$\left\langle \text{tr}_\sigma \left[\mathcal{T} e^{-\int_0^\beta d\tau (i\lambda \dot{\phi}_\tau \sigma_z + \gamma \sigma_x)} \right] \right\rangle_{\text{path}}^{(2)} \approx -\lambda^2 e^{\beta\gamma} \sum_{k=1}^{\infty} \frac{\beta^2 S_k}{2} \frac{\beta\gamma}{k^2 \pi^2 + \beta^2 \gamma^2}. \quad (\text{S.33})$$

This explicitly shows that the sum over k is cut off at energies $\gg \gamma$.

SV. DERIVATION OF LARGE DIPOLE-MOMENT MODEL

In the main text, we discuss a second explicit model, which generalizes the two-level quantum dipole model to many dipoles. We here provide details on the derivation of the model, needed to reproduce Fig. 2.

As pointed out in the main text, we generalize from one to many dipoles, where the total polarization operator is $\hat{\Lambda} = \sum_k \lambda_k \sigma_z^{(k)}/2$. The intrinsic dynamics $\hat{\Gamma}$ still includes a tunneling between charge (dipole) configurations, but includes now in addition a dipole-dipole interaction $\Gamma = \sum_k \gamma_k \sigma_x^{(k)}/2 + \sum_{k,k'} J_{k,k'} \sigma_z^{(k)} \sigma_z^{(k')}/4$. This model can be easily solved under the simplifying assumption that all dipole moments be identical and oriented the same way with respect to the capacitor ($\gamma_k = \gamma$, $\lambda_k = \lambda$) and, in addition, let the dipole-dipole interaction not depend on the spatial separation between dipoles $J_{k,k'} = J$. Thus, Eq. (8) in the main text depends only on the total pseudo-spins, $S_\alpha = \sum_k \sigma_\alpha^{(k)}/2$ ($\alpha = x, y, z$), where the pseudo-spin magnitude (total dipole magnitude) $S^2 = S_x^2 + S_y^2 + S_z^2$ is a conserved quantity. Fixing the total pseudo-spin to the maximal value $S = K/2$, we can represent the large spin in the standard representation

$$S_z = \sum_{m=-S}^S m |m\rangle \langle m|, \quad (\text{S.34})$$

$$S_x = \frac{1}{2} \sum_{m=-S}^{S-1} \sqrt{(S+m+1)(S-m)} |m+1\rangle \langle m| + \text{h.c.} \quad (\text{S.35})$$

This matrix representation is used in generating the plots of Fig. 2.